Synthesis, co-crystal structure and characterization of pyrazinamide with *m*-hydroxybenzoic acid, *p*-hydroxybenzoic acid and 3,4-dihydroxy benzolic acid

Ming Lou · Shu-Hua Mao · Yang-Hui Luo · Peng Zhao · Bai-Wang Sun

Abstract We here reported a series of co-crystal structure of pyrazinamide (PZA) with *m*-hydroxybenzoic acid (MHBA), *p*-hydroxybenzoic acid (PHBA) and 3,4-dihydroxy benzolic acid (3,4-DHBA) and obtained three co-crystals (co-crystal **1**–**3**, respectively) under the same conditions. These crystal structures were characterized by single-crystal X-ray diffraction, IR spectra, thermogravimetric analyses, differential scanning calorimetry, and Raman spectrum analysis. The images of single crystal diffraction revealed that **1** was a 1:1 (PZA:MHBA) co-crystal, **2** was a 1:1 (PZA:PHBA) co-crystal, and **3** was a 1:1 (PZA:3,4-DHBA). The strong O–H···O, N–H···O hydrogen bonding interactions between PZA and hydroxyl-substituted benzoic acid primarily made the structure of co-crystals stabilized. Hirshfeld surface and fingerprint plots of the three co-crystals showed that the structures were stabilized by H···H, O–H···O, N–H···O C–H···π, and π···π intermolecular interactions.

Introduction

The design of co-crystals has attracted worldwide attention, especially in the fields of pharmaceutical because they offer new opportunities for improving some relevant chemical–physical properties of a drug and not affect its therapeutic effects [1–9]. Pharmaceutical co-crystals can be defined as molecular complexes comprised of active pharmaceutical ingredients and one or more pharmaceutically acceptable co-crystal formers [10–12], while the structure of them is often controlled by the

M. Lou · S.-H. Mao · Y.-H. Luo · P. Zhao · B.-W. Sun (✉)
College of Chemistry and Chemical Engineering, Southeast University, Nanjing 210096, People's Republic of China
e-mail: chmsunbw@seu.edu.cn

direction and selective reorganization of hydrogen or halogen bonds within the crystals [13]. Co-crystals present different characteristics because of the intermolecular interactions. For example, in the field of medicine, pharmaceutical co-crystals not only improves the physical properties and bioavailability of a drug but also have little influence on its therapeutic effects [5, 9].

In this study, we applied the co-crystal strategy to solid pyrazinamide (PZA) with hydroxyl-substituted benzoic acids (MHBA:*m*-hydroxybenzoic acid, PHBA:*P*-hydroxybenzoic acid and 3,4-DHBA:3,4-dihydroxy benzolic acid) and obtained three co-crystals (Scheme 1) [14–17]. These crystal structures were characterized by single-crystal X-ray diffraction, IR spectra, thermogravimeric analysea(TGA),

Co-crystal 1

Co-crystal 2
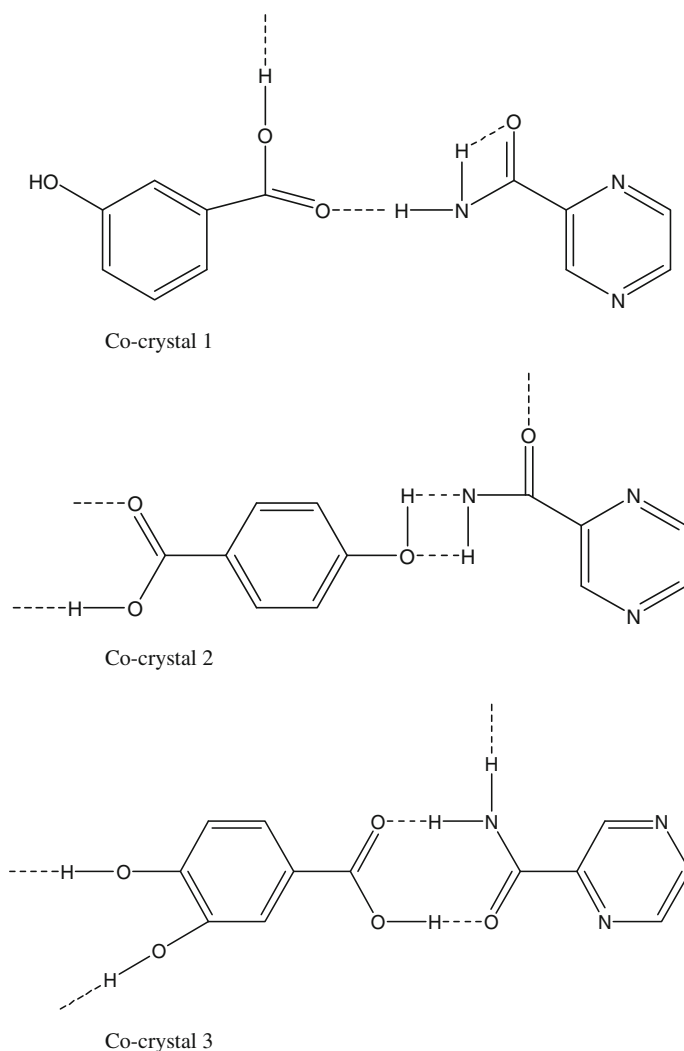
Co-crystal 3

Scheme 1 Structure of the three co-crystals, hydrogen bonds are shown as *dashed lines*

and differential scanning calorimetry (DSC), while we also made use of Hirshfeld surfaces analysis to research the intermolecular interactions of PZA with hydroxyl-substituted benzoic acids.

Experimental

General remarks

M-hydroxybenzoic acid (purity: 98 %, CAS registry number: 99-06-9), *p*-hydroxy-benzoic acid (purity: 99 %, CAS registry number: 99-96-7), 3,4-dihydroxy benzolic acid (purity: 97 %, CAS registry number: 99-50-3), PZA (purity: 99 %, CAS registry number: 5910-89-4), and all the other solvents (reagent grade) were commercially available and used as received without further purification.

Table 1 Crystal data and structure refinement for co-crystals **1–3**

	Co-crystal **1**	Co-crystal **2**	Co-crystal **3**
Empirical formula	$C_7H_6O_3$, $C_5H_5N_3O$	$C_7H_6O_3$, $C_5H_5N_3O$	$C_7H_6O_4$, $C_5H_5N_3O$
Formula weight	261.24	261.24	277.24
Wavelength (A)	0.71073	0.71073	0.71073
Crystal system	Orthorhombic	Orthorhombic	Triclinic
Space group	Pbca	Pca2$_1$	P−1
a (Å)	7.0712 (14)	28.918 (6)	6.9830 (14)
b (Å)	11.093 (2)	7.4182 (15)	11.06992)
c (Å)	32.014 (6)	11.303 (2)	16.590 (3)
α (°)	90.00	90.00	79.63
β (°)	90.00	90.00	77.92
γ (°)	90.00	90.00	89.98
V (Å^3)	2511.2 (8)	2424.7 (8)	1232.7 (4)
Z	8	8	4
T/K	293	293	293
Density (calculated), g cm^{-3}	1.382	1.431	1.494
Absorption coefficient, mm^{-1}	0.106	0.110	0.119
h, k, l (min, max)	(−8,8), (−13,13), (−39,39)	(−37,37), (−9,9), (−14,14)	(−8,8), (−13,13), (−19,19)
Parameters	174	348	367
F(000)	1,088	1,088	576
Goodness-of-fit on F2	1.056	1.046	0.985
Final R indices [I > 2σ(I)]	R1 = 0.1258	R1 = 0.0952	R1 = 0.1118
	ωR2 = 0.2714	ωR2 = 0.2353	ωR2 = 0.2507
CCDC No.	919366	919367	942698

Synthesis of co-crystal **1–3**

The synthesis of the co-crystals was carried out in solution crystallization experiments. Co-crystal **1** was obtained by the following procedure: stoichiometric amounts of PZA (0.5 mmol, 61.5 mg) and MHBA (0.5 mmol, 69.1 mg) were dissolved separately in a beaker with 10 ml of methanol solution, then combined and slowly evaporated at room temperature. A week later, we got club-shaped colorless crystals (yield 91 % based on MHBA). Mp: 141 °C. IR (KBr pellet, cm^{-1}): 3,434, 3,142, 1,704, 1,648, 1,450, 1,403, 1,300, 1,244, and the Raman spectrum characteristic peak: 3,078, 1,026, 997, 816, 773, 243. The synthetic steps of crystal **2**, crystal **3** and crystal **1** are similar including the solvent (yield 87 % based on PHBA). Mp: 172 °C. IR (KBr pellet, cm^{-1}): 3,417, 3,157, 1,704, 1,601, 1,403, 1,291, 1,168 and the Raman spectrum characteristic peak: 1,608, 1,275, 1,172, 846, 830, 638, (yield 92 % based on 3,4-DHBA). Mp: 174 °C. **IR** (KBr pellet, cm^{-1}): 3,520, 3,252, 1,815, 1,701, 1,500, 1,310, 1,244, and the Raman spectrum characteristic peak: 2,420, 1,100, 990, 793, 566, 475, respectively.

Thermoanalysis of co-crystals

The three co-crystals were characterized by TGA and DSC which were produced by Mettler–Toledo and conducted with the TGA/DSC STARe System at a heating rate of 10 K min^{-1} under an atmosphere of dry N$_2$ flowing at 20 cm^3 min^{-1} over a range from 40 to 300 °C.

X-Ray crystallographic study

Single-crystal X-ray diffraction analysis was performed for the three crystals **1–3** to determine their structures [18]. The crystals were selected and mounted in air onto thin glass fibers. Accurate unit cell parameters were determined by a least-squares fit of 2θ values and intensity datasets were measured on a Rigaku Raxis Rapid IP diffractometer with Mo–Kα radiation ($\lambda = 0.71073$ Å) at room temperature. The structure was solved using the SHELXS-97 package and refined with SHELXL-97 [19]. All non-hydrogen atoms were refined anisotropically. All hydrogen atom bonds to carbon, nitrogen and oxygen atoms were placed geometrically and refined isotropically. Full crystallographic details were collected in Table 1.

Hirshfeld surfaces analysis

Hirshfeld surfaces facilitate a novel method of visualizing intermolecular interactions by color-coding short or long contacts while the color intensity indicates the relative strength of the interactions. Additionally, the size and shape of a Hirshfeld surface also reflects the interplay between different atoms and intermolecular contacts in a crystal. The 2-D fingerprint plots, which are derived from the Hirshfeld surfaces, complement these. They quantitatively summarize the nature and type of intermolecular contacts experienced by the molecules in the crystal. Each point on the standard 2-D graph represents a bin formed by discrete intervals of de and di,
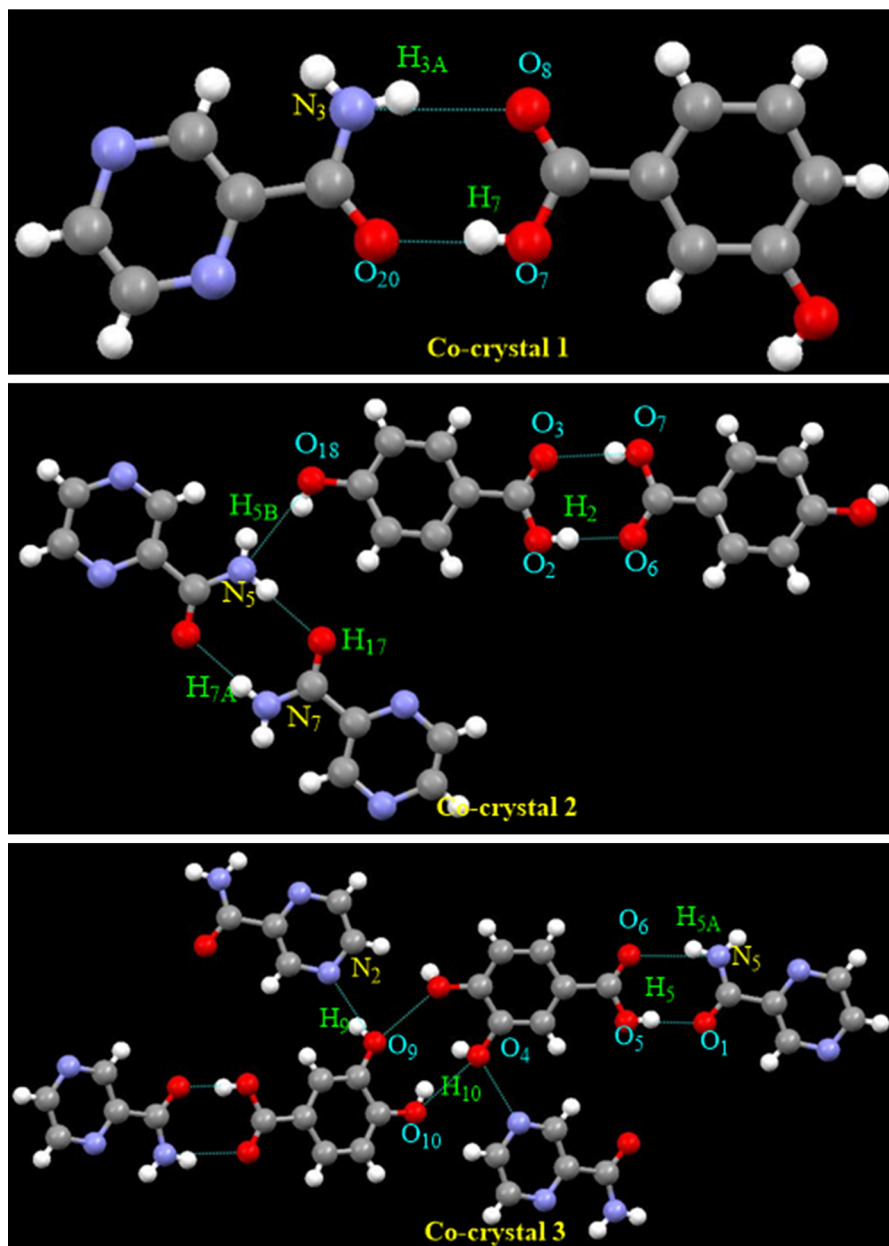
Fig. 1 The ball and stick model structure of the three co-crystals and the hydrogen bonds are shown as *dashed lines*

and the points on the surfaces are colored as a function of the fraction of the surface points in the bin [20]. For instance, the blue color indicates relatively few points while the green color means moderate points and the red color suggests many
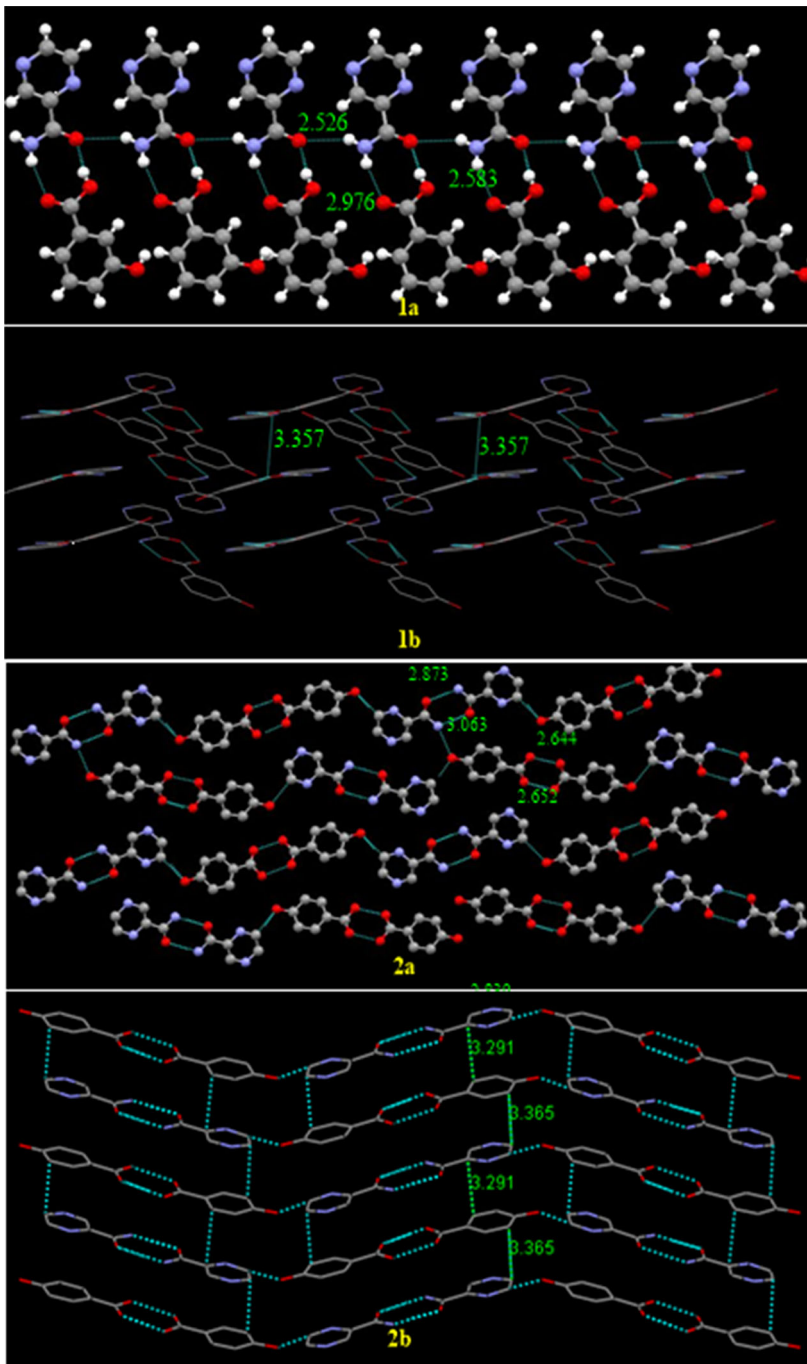
Fig. 2 *1a*, *2a* and *3a* are 1-D structures of co-crystals **1**, **2** and **3**, respectively; *1b*, *2b* and *3b* are 3-D pack structures of co-crystals **1**, **2** and **3**; the distance is indicated within hydrogen bond
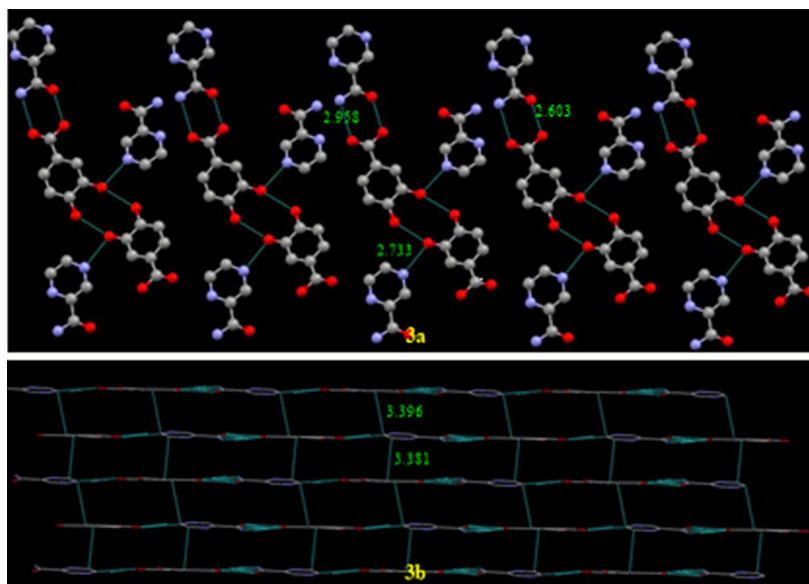
Fig. 2 continued

points. The 2-D fingerprint plots can also be broken down to give the relative contribution to the Hirshfeld surface area of each type of interaction present, quoted as the ''contact contribution''. For a given crystal structure, the Hirshfeld surfaces as well as the fingerprint plots are all unique [21], and the number of unique Hirshfeld surfaces depends on the number of crystallographically independent molecules in the corresponding asymmetric unit [22].

Results and discussion

Crystal structures of co-crystals **1–3**

We obtained three co-crystals from crystallization experiments through the reaction of PZA with hydroxyl-substituted benzoic acid at a molar of 1:1 in methanol solution; the diffraction data of the three co-crystals were collected at room temperature [23].

Co-crystal **1** crystallizes as colorless club-shaped crystals. The structure determination shows that **1** forms a 1:1 (PZA:MHBA) co-crystal in the orthometric Pbca space group with $Z = 8$. PZA and MHBA moleculars were connected by N–H⋯O (distance of 2.976 Å) (Fig. 2 1a) and O–H⋯O (distance of 2.583 Å) hydrogen bond. The PZA molecules are also stabilized by intramolecular N–H⋯O hydrogen bonds (distance of 2.526 Å), and the structure of PZA molecule and MHBA molecule are further stacked by π⋯π intermolecular interactions, with distances of

3.357 Å (Fig. 2 1b). The hydrogen bonds of the three co-crystals are summarized in Table 2 and Fig. 1. As shown in crystal **1**, co-crystal **2** also crystallizes as colorless club-shaped crystals which the structure determination shows that **2** forms a 1:1 (PZA:PHBA) co-crystal in the orthometric Pca2$_1$ space group with $Z = 8$. PZA and PHBA moleculars were connected by N–H···O hydrogen bonds (distance of 3.063 Å). The PZA molecules are also stabilized by a pair of intramolecular N–H···O hydrogen bonds (distances of 2.839 and 2.873 Å) (Fig. 2 2a), while the PHBA molecules are also stabilized by a pair of intramolecular O–H···O hydrogen bonds (distance of 2.652 and 2.644 Å) (Fig. 2 2a). The plane separations between PZA and PHBA molecules are 3.291 and 3.365 Å, respectively (Fig. 2 2b).

Unlike co-crystals **1** and **2**, co-crystal **3** crystallizes as light yellow club-shaped crystals and the structure determination shows that **3** forms a 1:1 (PZA:3,4-DHBA) co-crystal in the triclinic p–1 space group with $Z = 4$. PZA and 3,4-DHBA molecules were connected by N–H···O (distance of 2.958 Å) (Fig. 2 3a) and O–H…O (distance of 2.603 Å) hydrogen bond. The structure of PZA molecule and 3,4-DHBA molecule are further stacked by π···π intermolecular interactions, with

Table 2 Geometrical parameters for the hydrogen bonds in co-crystals **1–3**

D–H···A	D–H (Å)	H···A (Å)	D···A (Å)	<D–H···A (deg)
Co-crystal 1				
N3–H3A···O8	0.86	2.15	2.976	159.9
O7–H7···O20	0.82	1.78	2.583	166.7
N3–H3B···O20	0.86	2.54	3.309	150.2
Co-crystal 2				
O1–H1···N7	0.82	2..270	3.077	168.03
O2–H2···O6	0.82	1.918	2.652	148.58
O7–H7···O3	0.82	1.825	2.644	178.03
O18–H18···N5	0.82	2.342	3.062	147.00
N5–H5A···O17	0.86	1.984	2.839	172.90
N5−H5B···O18	0.86	2.346	3.062	140.97
N7–H7A···O12	0.86	2.018	2.873	172.83
N7–H7B···O1	0.86	2.365	3.077	140.46
Co-crystal 3				
O5–H5···O1	0.82	1.77	2.576	167
N5–H5A···O6	0.86	2.14	2.953	158
N5–H5B···O2	0.86	2.54	3.315	151
N6–H6A···O7	0.86	2.13	2.955	160
N6–H6B···O1	0.86	2.53	3.32	153
O8–H8···O2	0.82	1.82	2.604	158
O9–H9···N2	0.82	2.06	2.752	142
O10–H10···O4	0.82	2.12	2.817	142

distances of 3.396 and 3.381 Å (Fig. 2 3b). The packing structures of PZA molecules and guest molecules are spaced from each other.

Differential scanning calorimetry (DSC) and thermogravimetric analysis (TGA) of cocrystal 1-3

Differentical scanning calorimetry (Fig. 3a) and thermogravimetric analysis (TGA; Fig. 3b) were used to investigate the behaviors of the three crystals. The DSC patterns of co-crystals **1–3** show the effect of guest molecules to the PZA molecule on the melting point. For co-crystal **1**, we find there is only one endothermic peak at 140 °C. For co-crystals **2** and **3**, they have almost the same endothermic peaks: 172 and 175 °C, respectively. TGA thermograms of the three crystals show they have mass loss only once: 93.51, 90.78, and 88.64 %, respectively, and the PZA molecule and guest molecules show sublimation at the same time.

Hirshfeld surfaces analysis

The three-dimensional Hirshfeld surfaces and two-dimensional fingerprint plots of the PZA molecules in the three co-crystals are illustrated in Fig. 4, which shows surfaces that have been mapped over d_{norm} (−1.3 to 1.2, −0.81 to 1.4 ,and −0.83 to 1.2 Å for co-crystals **1**, **2** and **3**, respectively). It is clear that the information present in Table 3 is summarized effectively in these spots. The red color point in the 2-D
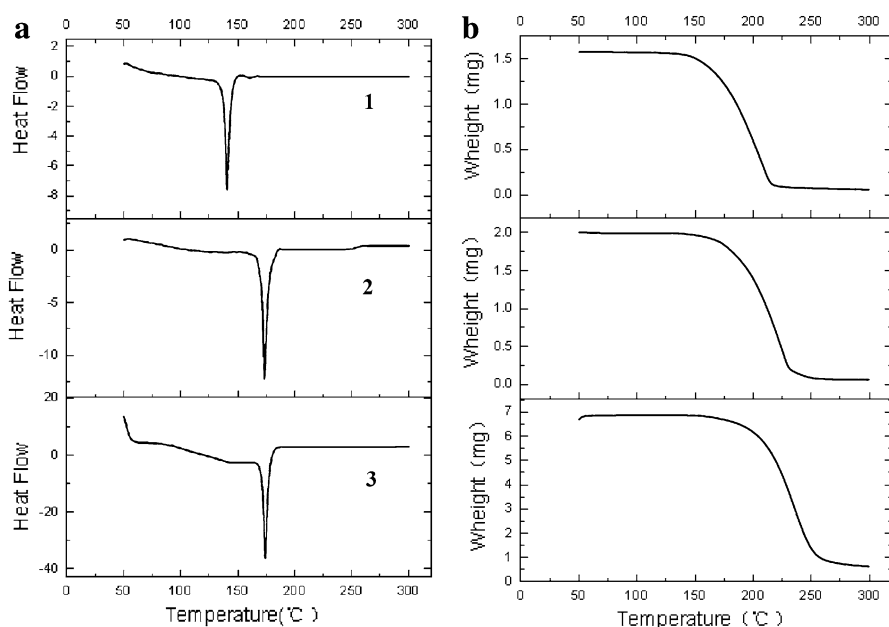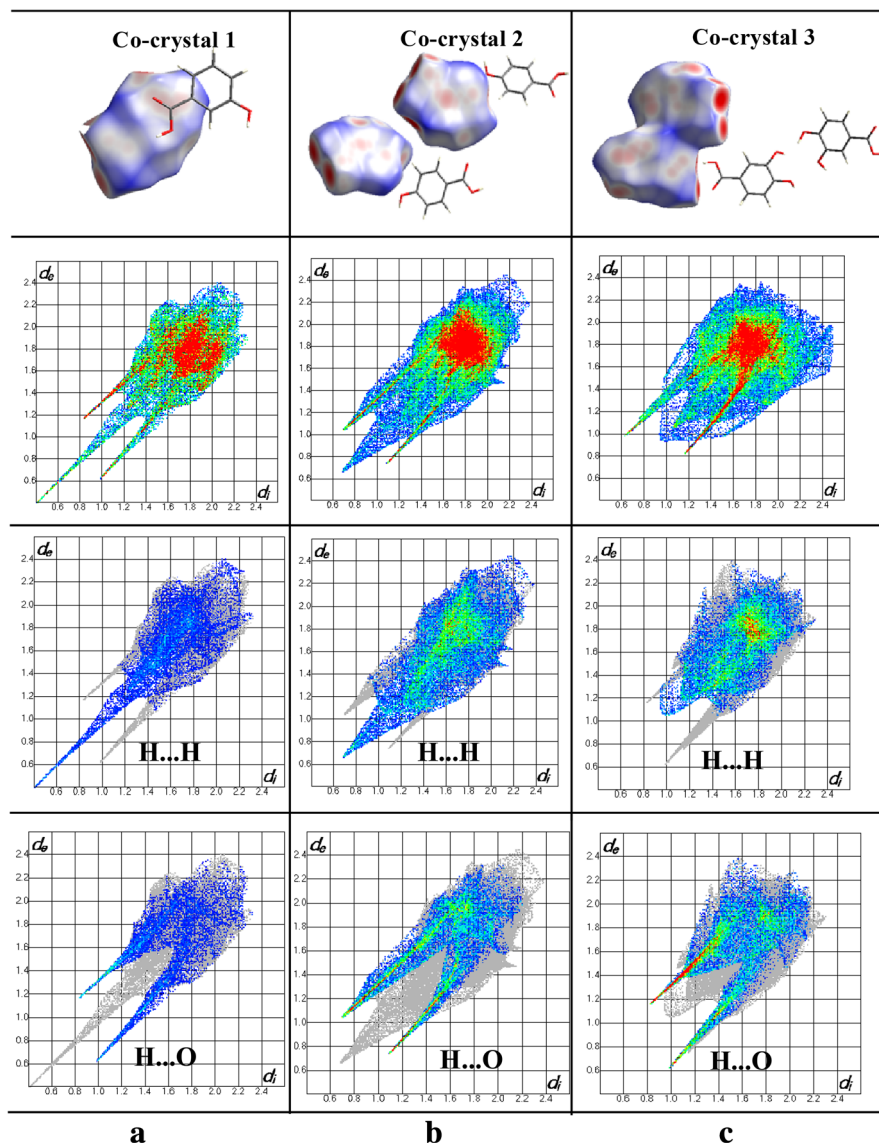

Fig. 3 The DSC and TGA profiles of co-crystals **1–3**

Fig. 4 Hirshfeld surfaces analysis of PZA in co-crystals **1–3** (*upper*) and the fingerprint plots for the three co-crystals resolved into H···H, H···O, and H···N interactions (*lower*)

fingerprint plots of co-crystals **1–3** on the d_{norm} surfaces correspond to H···H, H···N, and H···N interactions. In the co-crystal **1** (Fig. 4a), the H···H interactions appear as a sharp knife which makes the most significant contribution to the total Hirshfeld surfaces (28.5 %) and the H···H interactions in the 2-D fingerprint of co-crystal **1** is different from that of co-crystal **2** and co-crystal **3**, but the H···O interactions in the

Table 3 Summary of the various contact contributions to the PZA Hirshfeld surface area in co-crystals **1**–**3**

	Co-crystal **1**	Co-crystal **2**	Co-crystal **3**
H⋯H	28.5	32.6	29.5
H⋯O	23.1	21.8	25.6
N⋯H	17.8	11.6	15.2
C⋯H	8.9	7.2	8.6
C⋯C	5.1	7.8	5.7
C⋯O	7.0	4.4	8.0
C⋯N	2.7	5.1	2.3
N⋯N	0.9	1.1	0

2-D fingerprints of the three co-crystals are similar. The H⋯O intermolecular interactions look like a fork, which comprises 23.1 % of the total Hirshfeld surfaces, while N⋯H interactions play an important role in contributing to the total Hirshfeld surfaces (17.8 %). The C–H⋯π, C⋯C, and C⋯O interactions are in the corner of the 2-D fingerprint plot, and comprise 8.9, 5.1, and 7.0 %, respectively, of the total Hirshfeld surfaces. The Hirshfeld surfaces analysis for PZA in co-crystal **2** is displayed in Fig. 4b. The H⋯H interactions make the most significant contribution to the total Hirshfeld surfaces (32.6 %), and the H⋯O intermolecular interactions comprise 21.8 % of the total Hirshfeld surfaces, while H⋯N interactions play an important role in contributing to the total Hirshfeld surfaces (11.6 %). The C–H⋯π, C⋯C, and C⋯O interactions are in the corner of the 2-D fingerprint plot, and comprise 7.2, 7.8, and 4.4 %, respectively, of the total Hirshfeld surfaces.

The Hirshfeld surfaces analysis for PZA in co-crystal **3** (Fig. 4c) is similar to co-crystal **1**. For example, the H⋯H interactions are still the main contributor to the total Hirshfeld surfaces (29.5 %), amounting to 28.5 % for co-crystal **1**, while the H⋯O intermolecular interactions comprise 21.8 % of the total Hirshfeld surfaces. For co-crystal **2** it is 25.6 %, with the H⋯N interactions contributing 15.2 % to the total Hirshfeld surfaces. The C–H⋯π, c⋯c, and c⋯o interactions are in the corner of the 2-D fingerprint plot, and comprise 8.6, 5.7, and 8.0 % to the total Hirshfeld surfaces, respectively. The details of the main intermolecular interactions of three co-crystalsare shown Fig. 5.

Conclusions

We have investigated the detailed co-crystal formation of liquid PZA with co-crystal formers of hydroxyl-substituted benzoic acid (MHBA:*m*-hydroxybenzoic acid, PHBA:*p*-hydroxybenzoic acid, and 3,4-DHBA:3,4-dihydroxy benzolic acid). In addition, we make use of a new analysis method: the Hirshfeld surfaces and fingerprint plot analyses. With this method, we can not only detail the
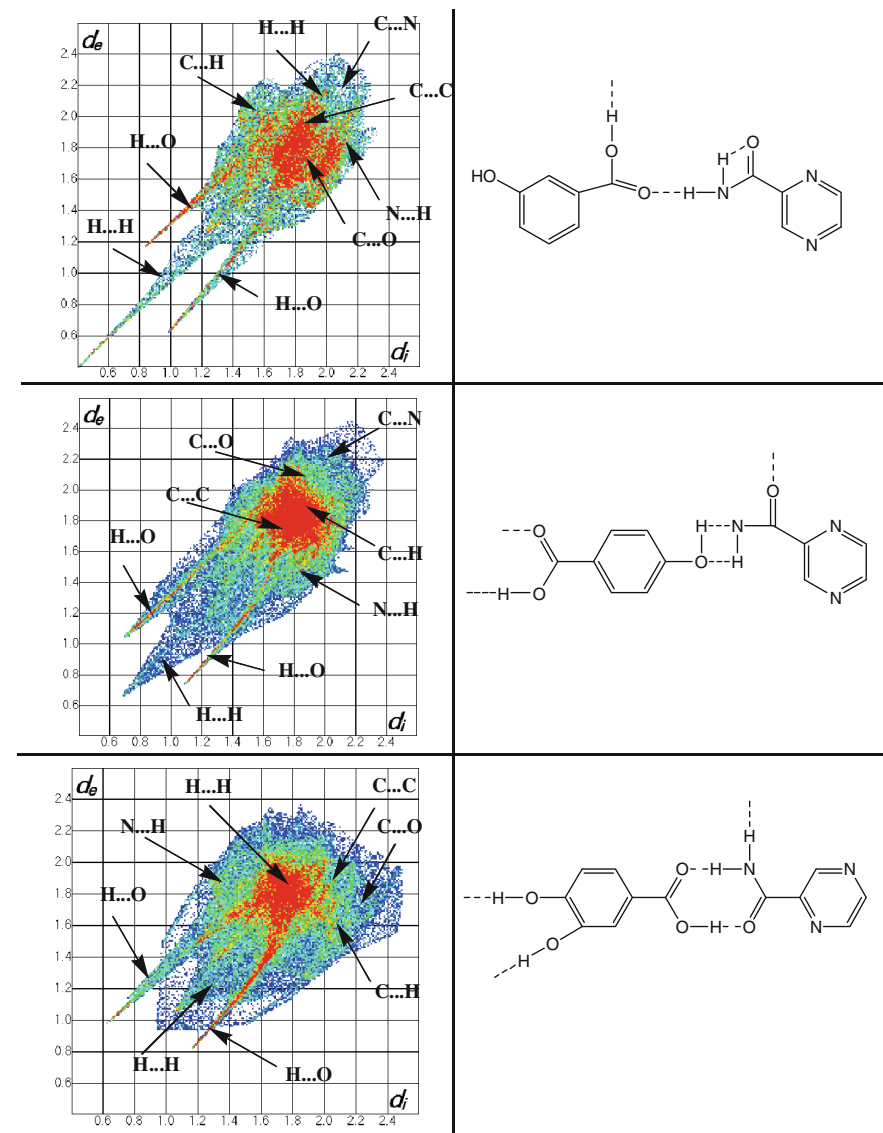
Fig. 5 The two-dimensional fingerprint of these co-crystals (*left*) and the structure of PZA in co-crystals 1–3 (*right*)

intermolecular interactions of pyrazinamide molecules in the three co-crystals but also know which kind of interactions contributes most to their stabilization.

References

1. R. Caliandroa, G.D. Profio, O. Nicolotti, J. Pharm. Biomed. Anal. **10**, 78–79 (2013)
2. Y.H. Luo, B.W. Sun, Cryst. Growth Des. **13**(5), 2098–2106 (2013)
3. O. Almarsson, M. J. Zaworotko, Chem. Commun. 1889–1896 (2004)
4. Y.H. Luo, B. Xu, B.W. Sun, J. Cryst. Growth (2013). doi:10.1016/jjcrysgro.201303007
5. C.B. Aakeroy, D.J. Salmon, Cryst. Eng. Commun. **7**, 439–448 (2005)
6. Y. H. Luo, G. G. Wu, B. W. Sun, J. Chem. Eng. D. (2013) doi: http://dx.doi.org/10.1021/je3011997
7. S.G. Fleischman, S.S. Kuduva, J.A. McMahon, B. Moulton, R.D.B. Walsh, N. Rodr_ıguez-Hornedo, M.J. Zaworotko, Cryst. Growth Des. **3**, 909–919 (2003)
8. Y.H. Luo, Y.R. Tu, J.L. Ge, B.W. Sun, Sep. Sci. Technol. (2013). doi:10.1080/014963952013.780256
9. S.L. Childs, L.J. Chyall, J.T. Dunlap, V.N. Smolenskaya, B.C. Stahly, G.P. Stahly, J. Am. Chem. Soc. **126**, 13335–13342 (2004)
10. G.R. Desiraju, Angew. Chem. **107**, 2541 (1995)
11. G.R. Desiraju, Angew. Chem. Int. Ed. Engl. **34**, 2311 (1995)
12. L.R. MacGillivray, J. Org. Chem. **73**, 3311 (2008)
13. T. Friščic, W. Jones, Cryst. Growth Des. **9**, 1621 (2009)
14. Y.H. Luo, Q. Zhou, B.W. Sun, J. Chem. Res. **36**(9), 506–509 (2012)
15. Y.H. Luo, J. Xu, B.W. Sun, J. Chem. Res. **36**(12), 697–700 (2012)
16. Y.H. Luo, G.G. Wu, S.L. Mao, B.W. Sun, Inorg. Chim. Acta **397**, 1–9 (2013)
17. Y.H. Luo, Y.T. Ma, Q.Q. Bao, B.W. Sun, J. Chem. Crystallogr. **42**, 628–632 (2012)
18. Y.H. Luo, C.G. Zhang, B. Xu, B.W. Sun, Cryst. Eng. Commun. **14**, 6860–6868 (2012)
19. G.M. Sheldrick, *SHELXL-97: Program for the Refinement of Crystal Structures* (University of Gottingen, Germany, 1997)
20. M.A. Spackman, J.J. McKinnon, Cryst. Eng. Commun. **4**, 378–392 (2002)
21. J.J. McKinnon, M.A. Spackman, A.S. Mitchell, Acta Crystallogr. Sect. B. **60**, 627–668 (2004)
22. J.J. McKinnon, F.P.A. Fabbiani, M.A. Spackman, Cryst. Growth Des. **27**, 75 (2007)
23. Z.C. Liu, M. Frasconi, J.Y. Lei et al., Nat. Commun. **4**, 1855 (2013)